MADRID
inter.noise 2019
June 16 - 19
NOISE CONTROL FOR A BETTER ENVIRONMENT

Engine noise source placement for shielding calculation

Marc Koch[1]
German Aerospace Center (DLR), Institute of Aerodynamics and Flow Technology, 37073 Göttingen, Germany

Lothar Bertsch[2]
German Aerospace Center (DLR), Institute of Aerodynamics and Flow Technology, 37073 Göttingen, Germany

Shielding the fan sound is a key element to further reduce aircraft noise immission of future aircraft designs. In recent studies the engine is represented as a single point source within scientific aircraft noise prediction tools, which can be a good approximation. In most low noise concept studies the engine is mounted above the wing or above the fuselage. The attenuation depends on the engine chordwise position due to the fact that either the fan forward noise or the fan aft noise is significantly shielded by the wing. The investigated simulation approach models the engine noise shielding more realistic by splitting the engine noise source into two noise sources. Herein one noise source is placed at the engine inlet position and radiates the fan forward noise, while the second one is placed at the nozzle exit position and radiates the fan aft noise. Depending on the relative position of the noise source to the aircraft surface, the results of attenuation due to shielding can be improved. This study investigates the differences in the results of splitting approach compared to a single point source approach.

Keywords: Shielding, Engine noise, split engine noise source
I-INCE Classification of Subject Number: 13, 52, 76

1 NOMENCLATURE

Symbols

h	=	altitude [ft] or [m]
l_c	=	chord length [m]
l_i	=	distance from fan disc center to engine inlet [m]
l_n	=	distance from fan disc center to engine nozzle [m]
L_A	=	A-weighted sound pressure level
N_1	=	fan rotational speed [$\frac{1}{min}$]
r	=	radius [m]
T	=	thrust [kN]
v	=	airspeed [$\frac{m}{s}$]
x, y	=	x, y coordinate specified by indice [m] or [km], aircraft position [m]
γ	=	slope of the trajectory [°]
φ	=	polar emission angle [°]

[1] email: marc.koch@dlr.de, Ph.D. candidate
[2] email: lothar.bertsch@dlr.de

Indices

cb	=	cutback
fdc	=	fan disc center (position)
opt	=	optimal engine position [m]

Abbreviations

BBN	=	broadband noise
off	=	no simulation of shielding effects, single noise source
SEL	=	sound exposure level [dB]
sns	=	shielding simulation with single noise source
split	=	shielding simulation with split noise source

2 INTRODUCTION

One of the dominant noise sources of present aircraft architectures is the engine. In the past, the engine noise has been, and still is, reduced by increasing the bypass ratio, improving the fan design, and applying acoustic liners in the engine nacelle [1]. Another promising approach for new aircraft designs to further reduce engine noise immission is to shield the engine noise. This can be achieved by placing the engine above the fuselage or the wings [2]. The most promising engine position towards a low noise architecture has to be determined as early as within the preliminary aircraft design phase. In this design phase the designer has the most influence to adapt the aircraft design toward a low-noise architecture. The designer of such architectures optimizes the engine position to minimize the noise impact on the ground.

Noise immission predictions of preliminary aircraft designs are conducted with tools such as the *Parametric Aircraft Noise Analysis Module* (PANAM) [2]. PANAM is comprised of semi-empirical noise source models. Since the distance to the ground is high, it can be assumed that the whole aircraft noise is emitted from a single point source. A tool called SHADOW is used in order to predict the shielding of the engine noise by the airframe [3]. The shielding capability is calculated using a monopole source. SHADOW calculates the results within a few minutes while performing with good accuracy. Therefore, it is suitable to predict the shielding capability of an aircraft design in the preliminary design phase which is comprised of large number of design iterations. PANAM adds the noise attenuation to the fan noise emission which, per definition, comes with a specific source directivity.

This study tackles the assumption that the engine noise source is modeled as a single point source for shielding assessment. In reality, however, engines emit the fan forward noise at the engine inlet and the fan aft noise at the bypass nozzle.[1] Therefore, there are 1.5 to 2 fan diameters between these noise emission locations. The aircraft surface shields the engine's inlet and aft noise sources differently due to the selected emission locations with respect to the surface. If the shielding attenuation for a highly shielded single point source is applied to fan inlet and aft noise, it might result in an underprediction of the fan noise immission (i.e. overprediction of shielding). Therefore, this study investigates the differences in modeling the fan sound as one point source versus two point sources placed in the inlet and nozzle. PANAM and SHADOW are enhanced to consider individual shielding of the fan inlet and aft noise. This feature should be applied if both inlet and the fan aft noise are subject to shielding. Similar engine noise splitting with individually shielded fan sources was already applied to the D8 by De la Rosa Blanco and Hileman (NASA and MIT) [4]. They split the fan into two noise sources and placed them individually above the fuselage. The D8's engine inlet noise is highly shielded by the fuselage, while engine aft noise is allowed a free line

[1] Private conversation with Martin Staggat, DLR.

of sight to the ground, and is reflected by the horizontal stabilizer mounted on top of the vertical stabilizer of the twin-tail. The presented study systematically investigates the effect of engine noise source splitting along approach and departure trajectories in case the engine is mounted above the wing. Finally, the the effects of prevailing operating conditions on the predicted shielding influence on the noise immission are investigated. These operating conditions directly determine the noise source ranking (emission), geometric spreading and atmospheric propagation which will influence the overall effectiveness of any noise shielding attempt.

3 METHODS

The aircraft deployed in this study is the *V-0* architecture from DLR [2] (see Figure 1). This vehicle has been selected due to its low-noise characteristics with the least modifications compared to existing vehicles. It is a medium range tube-and-wing aircraft with engines

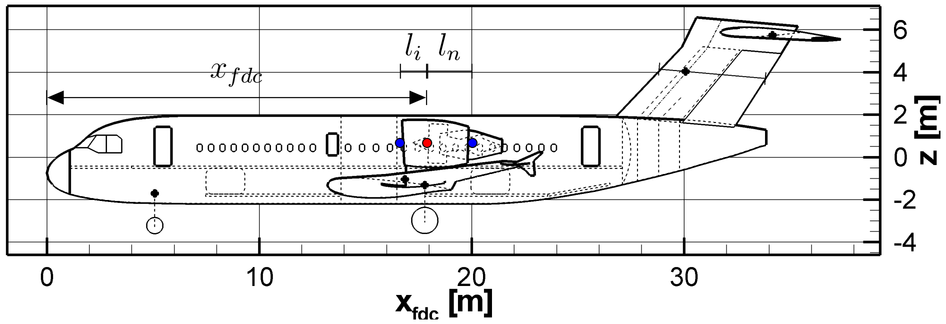

Fig. 1 – V-0 aircraft architecture with the point source in the fan disc center and the split noise source in the inlet and nozzle.

mounted above the wing to shield the fan sound. In earlier studies it has already been determined to have less noise impact towards the ground compared to the reference aircraft *V-R* from DLR [2, figure A63], which is a conventional tube-and-wing architecture with engines mounted underneath the wing. The aircraft design is calculated with *Preliminary Aircraft Design and Optimization* tool (PrADO), a software by University of Technology in Braunschweig [2, 5]. The mounted engine is calculated with GTlab [6] and based on the CFM56 engine, which is usually mounted on A320 and B737 sized aircrafts.

This investigation focuses on noise immission along representative operating conditions as experienced along typical approach and departure flights. In total, generic horizontal flyovers, three departures, and two landings[2] are investigated. The horizontal flyovers are simulated at different altitudes, thrust levels, and engine positions to study the influence of the atmospheric absorption, the duration due to altitude, the shielding influence, and the noise source ranking. The variation of the engine position influences the center of gravity location and the aerodynamic, hence affects the flight mechanics. Additionally a changed engine position might lead to heavier wing due to necessary reinforcing. With the focus on noise immission, these implications are neglected in this study. In addition to the generic flights, realistic departure and landing trajectories are assessed to identify the impact of the different shielding approaches under varying operating conditions. The flights are calculated with the software tool FlipNA [7]. The departures are simulated with full thrust at takeoff and a reduced engine speed after cutback ($N_{1,cb} = 86\%$, 90% and 94%) relative to the engine design point. All three departures show different noise source ranking, which becomes important for

[2]Landing is comprised of the descent sections, and the final approach.

the shielding efficiency. The selected descent angles along the two approach trajectories are in the range of typical approach procedures, including a steep approach.

The overall aircraft noise is simulated as a combination of multiple relevant noise sources: high-lift devices, gear, fan, and jet noise. Fan noise is divided into inlet and aft noise contribution. The applied noise source models are listed in Table 1. Due to this modular structure the

Table 1 – Noise sources and noise models used to predict aircraft noise emission.

noise source	**noise model**
fan inlet	Kontos fan noise model: buzz-saw, broadband and tones [8]
fan aft	Kontos fan noise model: broadband and tones [8]
jet	Stone jet noise model [9]
clean wing	DLR wing noise model [10]
leading edge	DLR leading edge noise model [10]
trailing edge	DLR flap noise model [10]
flap side edge	DLR flap side edge model [11]
landing gear	DLR landing gear noise model [10]

noise sources can be ranked at both the emission and immission. Best practice is to model the fan noise source as a single point source placed in the fan disc center (figure 1, red marker) [2, 12, 13]. Depending on the engine position, fan inlet sound, fan aft sound or both fan noise sources are shielded. For this study, PANAM was modified to consider individual fan noise shielding of the fan inlet and aft noise, which is radiated from the engine inlet and bypass nozzle (figure 1, blue marker). Due to their individual positions relative to the wing, the fan inlet and aft sound are shielded in different directions compared to a single point source located at the fan disc center. Table 2 summarizes the investigated types of shielding simulation concepts.

Table 2 – Investigated types of shielding simulation concepts and their abbreviations.

abbreviation	**shielding simulation concept**
off	no shielding (single point source)
sns	fan inlet and aft sound at fan disc center (single noise source)
split	fan inlet at $x_{fdc} - l_i$ and fan aft sound at $x_{fdc} + l_n$

A typical metric to assess aircraft noise is the A-weighted SPL. Consequently the A-weighted SPL and its corresponding integral metric SEL are selected to assess the flyover.

4 RESULTS

The following subsections describe the effect of different shielding simulation concepts as shown in Table 2 on the sound immission under various operating conditions. The simulated flights and the investigated effects are listed in Table 3. For the assessment of the horizontal flyovers (section 4.1), only fan sound is considered in order to to focus on only the basic correlations with respect to fan noise shielding. The selected departure (section 4.2) and approach (section 4.3) examples consider the overall aircraft noise. All presented thrust values and noise levels represent the overall aircraft (i.e. for two engines).

Table 3 – Investigated flights and effects.

simulated flight	investigated effects	numbering in text
generic	x_{opt} depending on shielding mode	①
	x_{opt} depending on thrust T	②
	Δ SEL depending on cutback rpm $N_{1,cb}$	③
	Δ SEL depending on the first descent angle γ_1	④
3 departures	SEL depending on $N_{1,cb}$	⑤
2 landings	SEL depending on γ_1	⑥

4.1 Generic test cases

Figure 2a shows the engine sound emission for two thrust settings (56 and 102 kN) at an altitude of $h = 2000$ ft. Different thrust settings are assessed because of a direct correlation between operating condition and noise source emission. The thrust settings have been selected to resemble operating conditions experienced along typical departures and approaches. During the 102 kN flyover, the engine's fan sound emission dominates towards the front, whereas during the 56 kN flyover the peak levels in the front and aft direction are roughly balanced. However, the peak directivity of the fan inlet sound emission changes from $\varphi \approx 50°$ at higher thrust to $\varphi \approx 40°$ at lower thrust. In the crucial emission directions of $50° \leq \varphi \leq 130°$, lower thrust results in level reductions for the fan inlet sound by 5 to 7 dB and fan aft sound by 2 to 3 dB. Therefore, the thrust reduction changes the noise source ranking and results in a dominating fan aft sound.

Figure 2c shows the shielding efficiency using *sns* and *split* simulation concepts at three altitudes and two constant thrust settings. $\Delta\text{SEL} = \text{SEL}_{shielded} - \text{SEL}_{off}$ is used to examine the shielding efficiency.[3] The solid line depicts the ΔSEL of the *sns* case and the dashed line of the *split* case. The following paragraphs investigate, first, the engine position with greatest shielding attenuation, second, the influence of thrust on the ΔSEL, and third, the influence of altitude on the ΔSEL.

First, the optimal engine positions according to the different shielding simulation concepts are investigated for different thrust settings and different flight altitudes.

The optimal engine position of the *split* case differs (① in Table 3) from the optimal *sns* case position. *Sns* exhibits an optimal position when having high shielding of inlet and aft noise, while in the *split* case, one has to find a compromise between high shielding of either the inlet or the aft noise source due to the engine length being relative to the chord length.

A different thrust setting leads to a new optimal engine position (② in Table 3). In the case of *split*, the maximum shielding is predicted assuming a forward shift of the engine position by 4 m at lower thrust and a backward shift by 2 m at higher thrust compared to the *sns*. The optimal position in the *sns* case is slightly moved upstream at lower thrust compared to the higher thrust case. Obviously, there is no one optimal position for all thrust settings, therefore a compromise is required. In general, the optimal location is tailored to the higher thrust case due to the higher maximum noise levels. At high thrust, the fan inlet sound, namely buzz-saw noise, dominates the fan sound emission, while at low thrust the fan aft sound dominates the fan sound emission. Hence, a selected engine position can only be optimal under a certain thrust setting.

Second, the influence of the thrust setting on the gained ΔSEL (③ in Table 3) is examined. In the *split* case, at the lower thrust, the achieved noise reduction is greater because the fan inlet noise is far below the fan aft noise, in addition to the fan aft noise being shielded very well. At higher thrust, fan inlet noise dominates slightly, thus the optimal engine posi-

[3] *shielded* can either be *sns* or *split*.

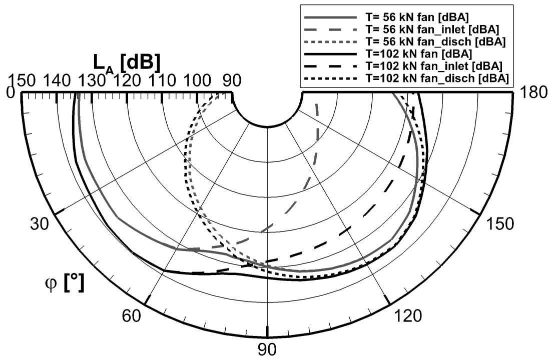

(a) Unshielded fan emission for different thrust settings of the overall aircraft (two engines).

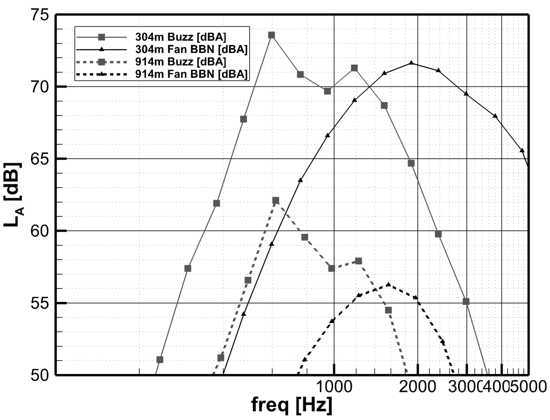

(b) Unshielded buzz-saw and fan aft broadband immission spectra.

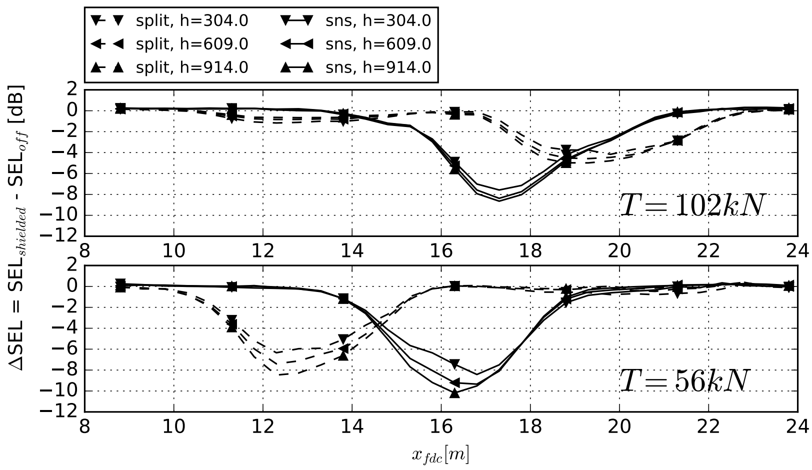

(c) ΔSEL values for split *and* sns.

Fig. 2 – (a) Emission (A-weighted, $r = 1\,m$) at $T = 56\,kN$ and $102\,kN$ thrust ($N_1 = 72\%$ and $N_1 = 87\%$) at $h = 2000\,ft$.
(b) Immission (A-weighted, $h = 1000\,ft$ and $3000\,ft$) at $T = 102\,kN$ and at two altitudes for the emission direction $\varphi = 90°$.
(c) Difference of $\Delta\mathrm{SEL} = \mathrm{SEL}_{shielded} - \mathrm{SEL}_{off}$ for a horizontal flyover at $T = 56\,kN$ and $102\,kN$ thrust and for different aircraft altitudes. Airframe and jet noise are not depicted. x_{fdc} is defined in Figure 1.

tion shields fan inlet noise, and fan aft noise can freely radiate to the ground. The *sns* case shows an additional reduction in fan noise compared to the *split* case. Indeed, in the *sns* case the high shielding values of the optimal location are applied to both fan noise sources.

Third, the influence of altitude on the noise reduction efficiency is investigated (④ in Table 3). The atmosphere attenuates the fan broadband noise (peak frequency at $2000\,\mathrm{Hz}$) more than the buzz saw noise (peak frequency at $800\,\mathrm{Hz}$), therefore both noise sources exhibit a similar noise immission level at $h = 1000\,\mathrm{ft}$, but a $5\,\mathrm{dB}$ difference at $3000\,\mathrm{ft}$ (Figure 2b). For a frequency of $2000\,\mathrm{Hz}$ the atmosphere attenuates $-8\frac{\mathrm{dB}}{\mathrm{km}}$, while for $500Hz$ it attenuates just $-2.4\frac{\mathrm{dB}}{\mathrm{km}}$ [14]. When the atmosphere attenuates most of the fan aft noise, the optimal engine position is the one, where the fan inlet noise is optimal shielded. This is the reason, why the $\Delta\mathrm{SEL}$ is approximately 1 to $3\,\mathrm{dB}$ greater at $3000\,\mathrm{ft}$ altitude compared to $1000\,\mathrm{ft}$ (Figure 2c).

For the detailed departure and approach investigations as presented in sections 4.2 and 4.3, the optimal engine positions as identified in section 4.1 are selected as followed: these are $x_{fdc} = 17.30\,\mathrm{m}$ in the *sns* case and $x_{fdc} = 19.80\,\mathrm{m}$ in the *split* case (Figure 2c).

4.2 Departure

Three departures are investigated (⑤ in Table 3), based on the results of the generic test cases. These departures are shown in Figure 3, along with their SEL immission predicted according to the investigated shielding simulation modes *split*, *sns*, and without any shielding. Different cutback rpm are investigated due to their huge impact on noise source ranking. Additionally, higher thrust levels results in faster altitude gain, hence, larger distances to the ground. Three departure trajectories with different rpm from $N_{1,cb} = 86\%$ to 94% are selected, which are representative cutback rpm along conventional departure procedures.

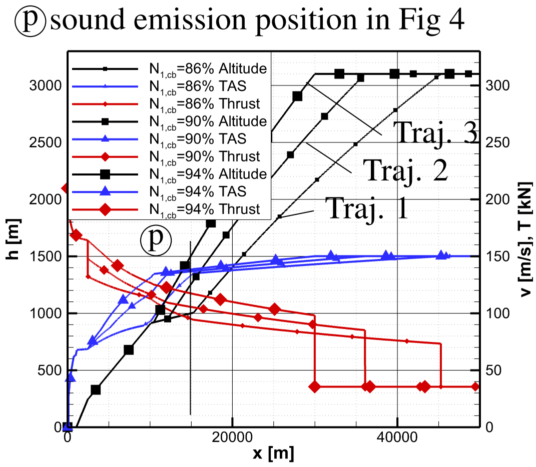

(a) Airspeed, altutude and thrust profiles.

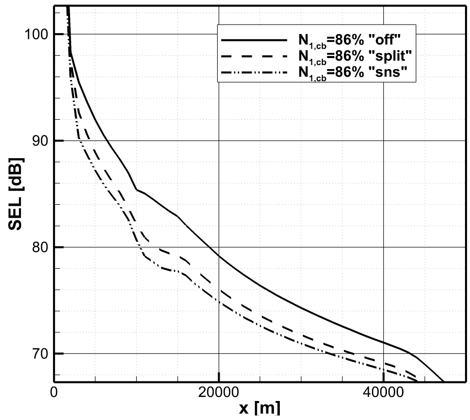

(b) SEL along flight ground track of Trajectory 1.

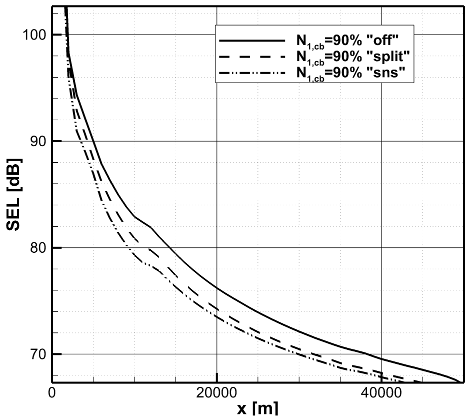

(c) SEL along flight ground track of Trajectory 2.

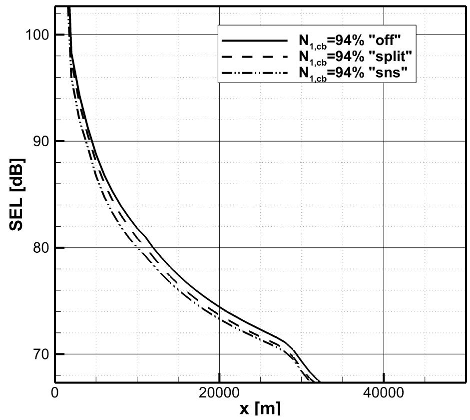

(d) SEL along flight ground track of Trajectory 3.

Fig. 3 – Departure trajectories and SEL immission for the three simulation cases.

First, the sound immission of the flights without shielding are compared to each other. After cutback, the SEL along the full thrust trajectory is about 4 to $5\,\mathrm{dB}$ lower for most of the flight compared to the low thrust trajectory. This can be attributed to the significant increase in altitude in combination with the decreased buzz-saw noise. The medium thrust trajectory is in between, thus about 2 to $3\,\mathrm{dB}$ below the noise immission of the low thrust trajectory. In this case, the slightly increased engine noise contribution along the medium thrust trajectory is outweighed by the increased distance to the ground.

Next, the sound reduction capability due to shielding is investigated for all trajectories. Along the higher thrust trajectory shielding reduces the SEL by 1 dB in the *split* case and 2 dB in the *sns* case. The overestimation of shielding effects caused by the *sns* simulation model now results in approximately 1 dB difference in predicted SEL along all the trajectories. According to Figure 3, the largest noise reduction due to shielding effects is predicted along the low thrust trajectory. What seems to be counterintuitive at first can directly be attributed to the source ranking. Along the low thrust trajectory, the fan inlet noise dominates the emission, Figure 4a. This fan source can be effectively shielded, while the other fan noise sources are reduced by the atmosphere. The least significant noise reduction due to shielding is predicted for the high thrust trajectory because here it is mainly the jet noise contributing to the SEL. Although jet noise does not seem to be dominant according to Figure 4d, it has to be noted that the atmosphere already attenuates $1000\,\text{Hz}$ with about $-4\frac{\text{dB}}{\text{km}}$ [14]. Therefore, high frequency noise contribution, e.g., fan aft and inlet noise, is strongly attenuated by the atmosphere. On the other hand, jet noise has a stronger impact on the SEL due to its long duration of immission according to the emission directivity. The directivity of the fan sound emission is to the front and back, while the jet emission is more omnidirectional up to $\varphi < 110°$ [9] under the prevailing operating condition and due to the A-weighting.

The engine sound emission during departure at $x = 15\,\text{km}$ behind the threshold is depicted in Figure 4. At all three operating points the fan inlet sound is dominated by the buzz-saw noise (Figure 4b). In case of the high thrust takeoff, fan inlet sound is $4\,\text{dB}$ lower compared to the medium and reduced thrust takeoff. This reduction with higher fan rpm comes from the fan noise model due to higher fan tip speeds [8]. While at $N_{1,cb} = 86\%$ fan inlet noise dominates the engine noise emission, at $N_{1,cb} = 90\%$ fan inlet and aft noise are balanced, and at $N_{1,cb} = 94\%$ the engine emission is dominated by fan aft noise. As a

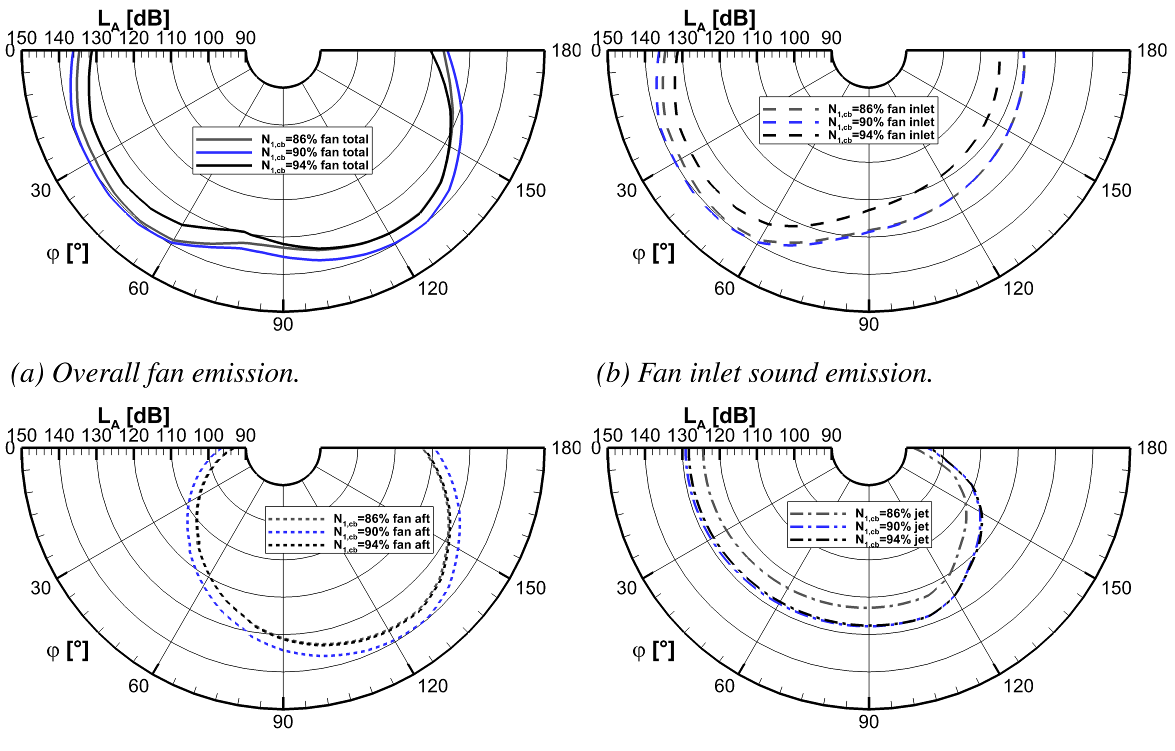

(a) Overall fan emission.

(b) Fan inlet sound emission.

(c) Fan aft sound emission.

(d) Jet sound emission.

Fig. 4 – Unshielded engine sound emission (A-weighted, two engines) at $N_{1,cb} = 86\%$ ($T = 94,8kN$, $h = 3280ft$), $N_{1,cb} = 90\%$ ($T = 105,5kN$, $h = 4150ft$) and $N_{1,cb} = 94\%$ ($T = 117,3kN$, $h = 4920ft$) at $x = 15km$.

consequence to this changing noise source ranking, fan noise shielding yields varying impact on the noise immission along the three trajectories. The fan aft sound emission of the low and high thrust trajectory remains at a similar level despite the fan speed and thrust being different in both operating points. On the medium thrust trajectory the fan aft sound is about 3 dB higher. Airframe sound can be neglected on all departure trajectories and the jet noise does not contribute to the SEL along the lower thrust trajectory.

4.3 Landing

Figure 5a shows the altitude, airspeed, and thrust along the selected conventional and steep approach trajectories (⑥ in Table 3). Along the steep approach, the high lift devices

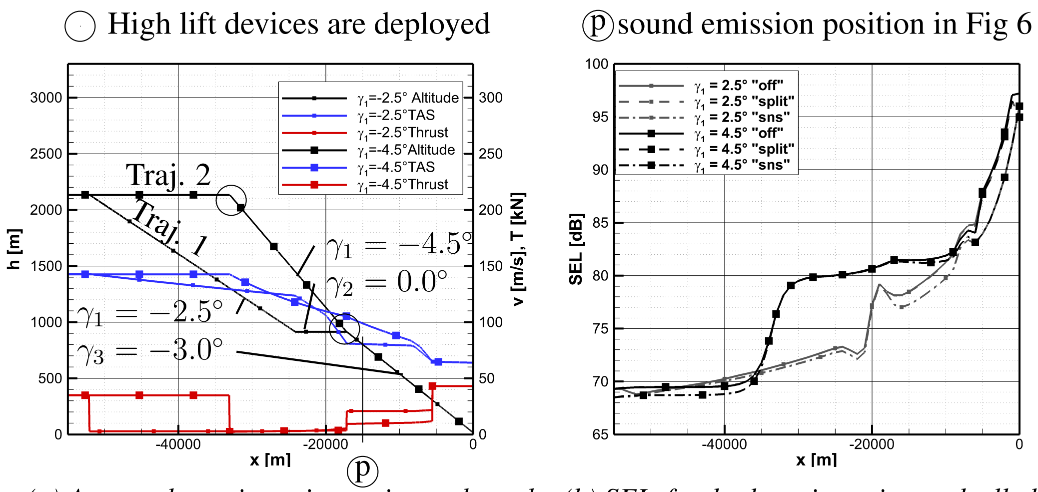

(a) Approach trajectories, airspeed and thrust.

(b) SEL for both trajectories and all three shielding cases.

Fig. 5 – Approach trajectories and SEL on ground track with $\gamma_1 = -2.5°$ and $-4.5°$ glideslopes.

are deployed early, around 33 km before the threshold, to decelerate the aircraft. This high lift device deployment causes the rise in noise immission starting at $x \approx -35$ km, while the noise immission of conventional approach rises just gradually along with the reduction of ground distance. At approximately $x \approx -20$ km the high lift devices are deployed upon the conventional approach to provide the required lift, which also causes increasing noise immission. Yet, the levels are still below the noise immission of steep approach due to a lower airspeed. This lower airspeed also results in a higher required thrust along the conventional approach to make up for the drag, while on the steep approach the aircraft still decelerates. Due to the higher thrust along the conventional approach the fan emits more noise, so that the reduction efficiency due to shielding *sns* on the conventional approach is higher than on the steep approach. The final leg is identical for both trajectories, leading to the same sound immission.

Consideration of shielding effects in the *split* mode does not show any impact on the SEL compared to no shielding at all. The shielding overestimation in the *sns* mode results in slightly increased noise reduction in sections along the flight path, in which the engine speed is above idle. If there is a difference in SEL_{split} and SEL_{sns} during the approach, then the fan aft sound dominates the sound emission. This is happening at around $x = -15$ km, where a large difference in the SEL can be observed between the two shielding methods and the two trajectories despite the fact that both trajectories result in similar flight altitudes of about $h = 1600$ ft in this region. According to Figure 6, assessment of noise emission at $x = -15$ km, this can be attributed to variations in airspeed and required thrust. Only fan and airframe are shown here as jet contribution can be neglected under the prevailing operating conditions. Along the steep approach, the airframe noise dominates in all directions due to

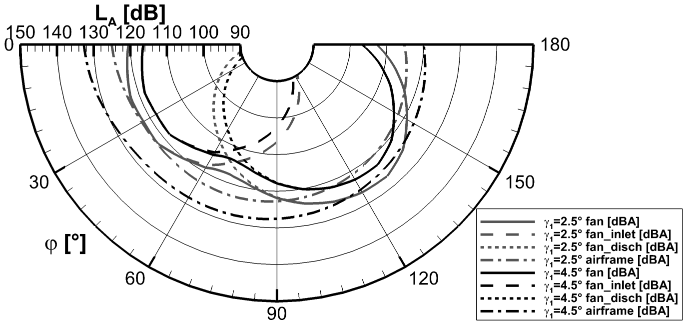

Fig. 6 – Airframe and unshielded engine sound emission (A-weighted) at $x = -15km$ for Trajectory 1 $\gamma_1 = -2.5°$ ($N_1 = 47\%$, $v = 80\frac{m}{s}$) and Trajectory 2 $\gamma_1 = -4.5°$ ($N_1 = 42\%$, $v = 99\frac{m}{s}$) glideslope.

the higher speed. As the fan aft noise is just 3 dB below the airframe noise, it also contributes to the overall noise emission in the aft directions. Along the conventional approach, fan inlet and airframe noise are balanced and fan aft noise dominates in the rearward direction. A predicted shielding influence can only be identified for the *sns* mode in which the fan aft noise is shielded. The nozzle is behind the wing's trailing edge, and radiates freely to the ground. Therefore an overestimation of the shielding is expected.

5 DISCUSSION

Different simulation approaches toward a more realistic depiction of the engine are investigated. The engine is represented as a single noise source (*sns*) versus a separate representation of the engine inlet and aft noise source (*split*). The predicted shielding influence is studied along generic horizontal flights, and along representative departure and landing trajectories using the emission (L_A) and the immission (SEL).

5.1 Generic test cases

The single point source representation leads to a higher predicted shielding capability, because the shielding performance of the single point source is applied to the overall fan sound emission. In the *split* case the noise sources are placed in the inlet and nozzle. If the chord length of the shielding surface is similar to the distance between fan inlet and bypass nozzle, inlet and aft noise will be affected differently by noise shielding. Consequently, the simulation mode *split* should be selected for over-the-wing aircraft, as studied here, or the shielding should only be applied to one of the two sources as demonstrated in [2].

If shielding is assessed for over-the-wing aircraft, an optimal engine position can be identified with maximum shielding efficiency. This optimal position depends on the thrust setting due to the noise source ranking. At high thrust, the fan inlet sound emission is greater than fan aft sound emission. At lower thrust the fan aft sound dominates, and the directivity of the fan inlet sound changes leading to more sound radiating toward smaller emission angles. The buzz-saw noise disappears due to the reduced fan speed. Therefore, the shielding concept should be maximized for fan inlet emission shielding under high thrust settings and for fan aft emission shielding under low thrust settings. Obviously, a compromise is required for the engine positioning to achieve maximum shielding for the most relevant operating condition.

Note that the predicted ΔSEL along the low thrust trajectory is slightly higher compared to the high thrust trajectory. This higher ΔSEL is due to the selected engine position featuring a large attenuation of fan aft noise as well as a low contribution of fan inlet noise.

5.2 Departure

During departure the engine dominates the noise immission. Ranking among the individual engine noise sources and the resulting emission directivity differs. In case of the low thrust trajectory, shielding has the greatest impact on noise reduction because the buzz-saw sound dominates the engine sound immission. Consequently, fan inlet noise shielding becomes most effective. The impact on noise immission in the vicinity of the ground track is shown in Figure 7. The contour areas in the *sns* case are shorter, and at the same time slightly

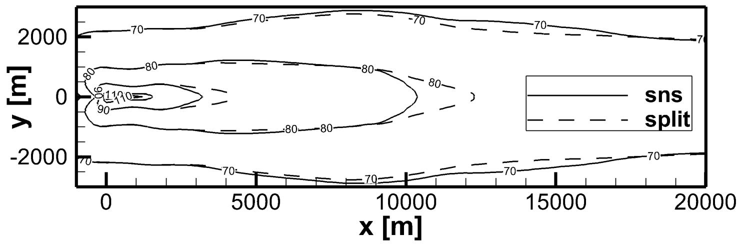

Fig. 7 – SEL [dB] immission on ground for the sns *(solid lines) and* split *(split lines) cases for the departure trajectory at* $N_{1,cb} = 86\%$.

wider compared to the *split* contour areas. The shorter areas can be attributed to the increased shielding as predicted by the *sns* mode. The slightly narrower areas in the *split* case can be attributed to the inlet sound source placed further downstream. Thus, it is better shielded to the side due to the swept wing. Keep in mind that this lower frequency noise is less attenuated by the atmosphere.

In case of the medium thrust trajectory buzz-saw sound and fan aft sound are on a similar level. While close to the ground, the fan aft sound immission is greater than the buzz-saw sound immission, at higher altitudes ($h > 1100\,\text{ft}$) it switches into a dominating buzz-saw sound due to atmospheric attenuation of the higher frequency fan aft sound. Shielding of the buzz-saw noise obviously becomes more efficient with increasing altitude.

On the high thrust trajectory the same change from dominating fan aft sound to dominating buzz-saw sound is seen at around $2100\,\text{ft}$. Nevertheless, on this trajectory the jet sound is dominating the sound immission and fan sound contributes just little to the SEL. Hence, any shielding will have less impact on the resulting SEL for the overall aircraft.

5.3 Landing

Along both investigated landing trajectories mainly the airframe noise contributes to the noise immission. In comparison to the takeoff, shielding makes only a minor contribution to the noise immission reduction, and shielding the fan inlet noise (*split* case) does not reduce the SEL because fan aft and airframe noise dominate the immission. Obviously, any shielding position would not be tailored to an approach but to a departure with dominating engine noise. If shielding shall be applied to reduce fan noise during approach, then the dominating fan aft sound should be shielded.

6 CONCLUSION

Two different simulation methods in the context of engine noise shielding are compared. A single noise source is compared to a split noise source, which represents the fan inlet and aft noise. This modification is also the basis for future work towards distributed propulsion concepts.

Significant differences can be expected, when the engine is only partially located above a shielding surface. A reference vehicle with the engines mounted above the wing has been selected to demonstrate this effect. This vehicle is assessed along generic flights and along typical approach and departure flights. Shielding effects are highly dependent on the frequency content and the directivity of the shielded noise source. Consequently, a detailed assessment has been initiated. The noise differences along typical approach flights are in the order of 0 to $1.5\,\text{dB}$ and along a typical departure the levels differ between 1 to $4\,\text{dB}$. Individual shielding can have a great impact on the noise immission, if the shielded noise source dominates. Especially with engines that are shielded by wings with a chord length longer than the engine length, splitting is worth considering. Based on the application examples, it can be concluded that the *sns* mode will result in an overprediction of shielding effects compared to the *split* mode if directly applied to the wing shielding example. To avoid this, predicted shielding effects by the *sns* mode should only be applied to one direction, forward or rearward noise, in case that only the engine inlet or aft sound is shielded. In cases in which only one of the two fan noise sources is shielded by a surface, the single source approximation with shielding of one of both sources is well suitable (e.g., see application examples in [2]).

REFERENCES

[1] M. J. T. Smith, *Aircraft Noise* (Cambridge University Press, Cambridge) (1989).

[2] L. Bertsch, “Noise prediction within conceptual aircraft design”, DLR Forschungsbericht, ISRN DLR-FB-2013-20 (2013).

[3] M. Lummer, *The Ray-Tracing Program SHADOW 0.9.7*, DLR, Brunswick (2009).

[4] E. De la Rosa Blanco and J. I. Hileman, “Noise assessment of the double-bubble aircraft configuration”, in *49th AIAA Aerospace Sciences Meeting including the New Horizons Forum and Aerospace Exposition*, January, 1–9 (AIAA, Orlando, Florida) (2011).

[5] W. Heinze, C. M. Österheld, and P. Horst, “Multidisziplinäres Flugzeugentwurfsverfahren PrADO - Programmentwurf und Anwendung im Rahmen von Flugzeug-Konzeptstudien”, (Deutscher Luft- und Raumfahrtkongress, Hamburg) (2001).

[6] R. G. G. Becker, F. Wolters, M. Nauroz, and T. Otten, “Development of a Gas Turbine Performance Code and its Application to Preliminary Engine Design”, in *Deutscher Luft- und Raumfahrtkongress (DLRK)* (Bremen) (2011).

[7] J. Blinstrub, L. Bertsch, and W. Heinze, “Assessment of the Noise Immission along Approach and Departure Flightpaths for Different SFB 880 Vehicle Concepts”, Number 0 in AIAA AVIATION Forum (AIAA) (2019).

[8] K. B. Kontos, B. A. Janardan, and P. R. Gliebe, “Improved NASA-ANOPP Noise Prediction Computer Code for Advanced Subsonic Propulsion Systems. Volume 1 ANOPP Evaluation and Fan Noise Model Improvement”, Technical Report 24, NASA (1996).

[9] J. R. Stone, D. E. Groesbeck, and C. L. Zola, “Conventional Profile Coaxial Jet Noise Prediction”, AIAA Journal **21**, 336–342 (1983).

[10] M. Pott-Pollenske, W. Dobrzynski, H. Buchholz, S. Guérin, G. Saueressig, and U. Finke, “Airframe Noise Characteristics from Flyover Measurements and Prediction”, in *12th AIAA/CEAS Aeroacoustics Conference* (AIAA, Cambridge, Massachusetts) (2006).

[11] K.-S. R. Rossignol, “Empirical prediction of flap tip noise”, in *17th AIAA/CEAS Aeroacoustics Conference*, June (AIAA, Portland, Oregon) (2011).

[12] P. Malbéqui, Y. Rozenberg, and J. Bulté, “AIRCRAFT NOISE PREDICTION IN THE IESTA PROGRAM”, ONERA Homepage (2009), description of CARMEN on the ONERA homepage.

[13] F. Centracchio, L. Burghignoli, M. Rossetti, and U. Iemma, “Noise shielding models for the conceptual design of unconventional aircraft”, (InterNoise, Chicago, Illinois) (2018).

[14] ISO 9613-1:1993(E) , “Acoustics - attenuation of sound during propagation outdoors”, (1993).